### Title
Electrical resistivity study of CeZn11: Magnetic field and pressure phase diagram up to 5 GPa




### Journal
Physical Review B, 88(19)

### ISSN
2469-9950



### Authors
Taufour, Valentin
Hodovanets, Halyna
Kim, Stella K
et al.



### Publication Date
2013-11-15

### DOI
10.1103/physrevb.88.195114

Peer reviewed

# Electrical resistivity study of $CeZn_{11}$: Magnetic field and pressure phase diagram up to 5 GPa

Valentin Taufour,[1,*] Halyna Hodovanets,[1,2] Stella K. Kim,[1,2] Sergey L. Bud'ko,[1,2] and Paul C. Canfield[1,2]

[1]*Department of Physics and Astronomy, Iowa State University, Ames, Iowa 50011, USA*

[2]*The Ames Laboratory, US Department of Energy, Iowa State University, Ames, Iowa 50011, USA*

(Received 19 August 2013; published 8 November 2013)

Thorough resistivity measurements on single crystals of $CeZn_{11}$ under pressure $p$ and magnetic field $H$ are presented. At ambient pressure, $CeZn_{11}$ orders antiferromagnetically at $T_N = 2$ K. The pressure dependence of the resistivity reveals an increase of the Kondo effect. We determine the pressure evolution of the magnetic exchange interaction between conduction and localized $4f$ electrons. It qualitatively reproduces the pressure evolution of the magnetic ordering temperature $T_{O_1}$ (with $T_{O_1} = T_N$ at ambient pressure). In addition to $T_{O_1}$, a new anomaly $T_{O_2}$ appears under pressure. Both anomalies are found to increase with applied pressure up to 4.9 GPa, indicating that $CeZn_{11}$ is far from a pressure induced quantum critical point. Complex $T$-$H$ phase diagrams are obtained under pressure which reveal the instability of the ground state in this compound.

DOI: 10.1103/PhysRevB.88.195114 PACS number(s): 75.30.Kz, 75.20.Hr, 72.15.Qm, 71.27.+a

## I. INTRODUCTION

Cerium based compounds have been extensively studied due to the existence of fascinating phenomena such as heavy fermion behavior, quantum criticality, and/or superconductivity.[1–4] The physics of these materials arises from a competition between different interactions such as the magnetic Ruderman-Kittel-Kasuya-Yosida (RKKY) interaction or the Kondo effect.[5,6] In the study of these materials, pressure and magnetic field were rapidly recognized as thermodynamic parameters that can be used to tune the interactions. Recently, we reported[7] the synthesis and physical properties of single crystals of $CeZn_{11}$. Such large coordination compounds often show strongly correlated electron behaviors,[8,9] or good thermoelectric properties.[10] In this paper, we report on the effects of pressure on single crystals of $CeZn_{11}$.

$CeZn_{11}$ was reported to crystallize in the tetragonal $BaCd_{11}$ structure type (space group $I4_1/amd$).[11] Each cerium atom is coordinated by 22 atoms of zinc. The cerium site has a tetragonal, noncentrosymmetric point symmetry ($D_{2d}$). A magnetic ordering occurs below 2 K and was attributed to antiferromagnetism from magnetization measurements.[7,12] Despite this relatively low antiferromagnetic ordering temperature, no strong signature of quantum fluctuations have been observed.[7] The effective moment $\mu_{\text{eff}} \approx 2.48\ \mu_B$/Ce is very close to the trivalent free ion value of 2.54 $\mu_B$/Ce for $Ce^{3+}$. The determination of the Sommerfeld coefficient $\gamma$ is ambiguous since no Fermi liquid behavior is observed in specific heat as well as in resistivity, at least above 0.4 K.[7] At 3 K, above the ordering temperature, the value of $C/T$ is larger than 1 J mol$^{-1}$ K$^{-2}$, whereas it is only 14 mJ mol$^{-1}$ K$^{-2}$ in $LaZn_{11}$. In fact, such large value does not arise from electronic correlations, but from the presence of a low lying crystal electric field (CEF) level. Such small CEF splitting is already known to give "false heavy fermion" behavior.[13] The value of $C/T$ is reduced to 100 mJ mol$^{-1}$ K$^{-2}$ below the ordering temperature, at 0.4 K. This value is still significantly larger than $\sim$10 mJ mol$^{-1}$ K$^{-2}$ obtained for $LaZn_{11}$.[7,12] When taking into account a CEF level at $E_1 \sim$ 10–12 K, a value of $\gamma \sim$ 35–43 mJ mol$^{-1}$ K$^{-2}$ was obtained.[7,12] In another Ce compound with large coordination, $CeCd_{11}$, a small $\gamma \sim 26$ mJ mol$^{-1}$ K$^{-2}$ was also found.[14] To the contrary, the case of the related compound, $UCd_{11}$ is reported to be a heavy fermion compound[15] with a $\gamma$ value as large as $\gamma \sim 840$ mJ mol$^{-1}$ K$^{-2}$ in the paramagnetic state (above 8 K) and 250 mJ mol$^{-1}$ K$^{-2}$ in the antiferromagnetic state (below 1 K). It should be noted, however, that recent de Haas-van Alphen studies[16] in $UCd_{11}$ (with a magnetic field $H > 6.5$ T) have revealed relatively small cyclotron masses in the range 1.6–7.2$m_0$ ($m_0$ is the rest electron mass) and an overall CEF splitting smaller than 100 K.[17]

The CEF splitting in $CeZn_{11}$ is among the lowest in cerium compounds, with the first excited level at $E_1 \sim$ 10–12 K from specific heat measurements.[7,12] A lower CEF splitting, with $E_1 = 6.7$ K, was observed in cerium ethylsulfate $Ce(C_2H_5SO_4)_3\ 9H_2O$.[18] In $CeCd_{11}$, $E_1 = 17.5$ K.[14,19] The CEF effect tends to reduce the single ion Kondo temperature by reducing the degeneracy of the ground state.[20–22]

Given the low ordering temperature, as well as the low CEF splitting in $CeZn_{11}$, pressure may result in significant changes in the low-temperature state, and ultimately is expected to lead to a quantum phase transition, possibly even a quantum critical point. In this paper, we present the results of measurements of electrical resistivity as a function of temperature and applied magnetic field under applied pressures up to 4.9 GPa.

## II. EXPERIMENTAL DETAILS

In the present study, several high-quality single crystals of $CeZn_{11}$ were used. The samples were grown from high-temperature binary solutions rich in zinc in the molar ratio Ce:Zn of 1.5 : 98.5, and characterized by x-ray Laue diffraction, resistivity, magnetization, and specific heat measurements as detailed in Ref. 7. The residual resistivity ratio [RRR$\equiv \frac{\rho(300\text{K})}{\rho(0.4\text{K})}$] is higher than 300, indicating the high quality of the samples. Pressure was applied using a modified Bridgman cell.[23] In such a cell, it is possible to use liquids as the pressure-transmitting medium. Pressures as high as $\sim$7 GPa can be obtained when using Daphne oil 7373[24] or Fluorinert.[23] In this study, we used a 1:1 mixture of $n$-pentane:isopentane, which is a more hydrostatic medium.[25,26] The solidification of this medium occurs at room temperature at $\sim$6–7 GPa.[25,27] However, this medium is more compressible and, as a result,

 

our pressure limit was reduced to ∼5 GPa. In order to ensure the sealing of the pressure cell, the initial pressure has to be larger than 2 GPa. The pressure was determined by measuring the superconducting transition of Pb resistively.[28] Electrical resistivity was measured down to 2 K and at fields up to 9 T in a commercial Quantum Design Physical Property Measurement System (PPMS), employing the four probe ac method with current parallel to the [1$\bar{1}$0] axis. Four gold wires (12 $\mu$m ø) were spot welded on the sample. Magnetic field was applied along the [110] axis, which corresponds to the magnetization easy axis.[7] Measurements down to 400 mK were performed in a $^3$He cryostat (CRYO Industries of America) with a LakeShore 370 ac resistance bridge. Knowledge of the sample geometry enabled us to estimate the absolute resistivity to within 15%.

## III. RESULTS

The temperature dependence of the electrical resistivity at different pressures is shown in Fig. 1(a). Increasing pressure is expected to move the energy of the 4$f$ electrons of cerium ions closer to the Fermi energy. This enhances the Kondo effect and therefore increases the magnetic scattering of the conduction electrons with the 4$f$ electrons, which explains the increase of the resistivity with pressure at low temperature (below 150 K).

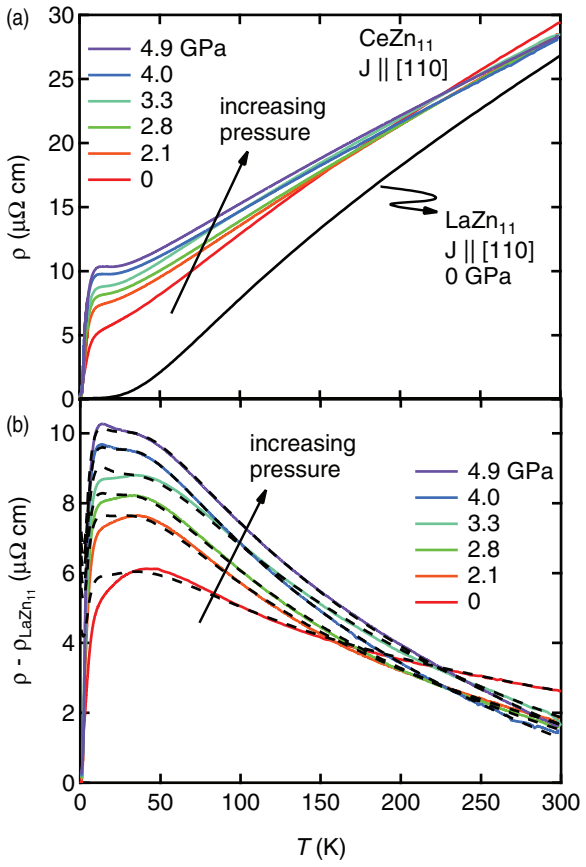


FIG. 1. (Color online) (a) Temperature dependence of the electrical resistivity of $CeZn_{11}$ at different pressures. The measurement on a $LaZn_{11}$ single crystal $\rho_{LaZn_{11}}$ is also shown. (b) Temperature dependence of $\rho - \rho_{LaZn_{11}}$ at different pressures. Dashed lines are fits from the Cornut and Coqblin model[20] (see text).

In addition, Fig. 1(a) shows that the ambient pressure broad shoulder in the resistivity around 15 K becomes more pronounced with applied pressure. The contribution of cerium ions to the electrical resistivity can be obtained by subtracting the resistivity of $LaZn_{11}$. The resistivity of a single crystal of $LaZn_{11}$ measured at ambient pressure with electrical current parallel to the [1$\bar{1}$0] axis is also shown in Fig. 1(a) (reproduced from Ref. 7). In this work, we assume that any pressure dependence of the $LaZn_{11}$ resistivity is negligible. The subtracted resistivity $\rho - \rho_{LaZn_{11}}$ (sometimes referred to as the magnetic resistivity) at different pressures is shown in Fig. 1(b). In fact, two broad anomalies (changes of slope) can be observed at ∼15 and ∼60 K. These features correspond to the energy of the CEF levels as determined from specific heat measurements at ∼12 and ∼65 K from Ref. 7 or at ∼10 and ∼48 K from Ref. 12. A similar influence of the CEF levels on the electrical resistivity can be observed in many other cerium based compounds.[29–41] The two anomalies we observe are expected to merge under pressure with the increase of the Kondo effect[42] and indeed, at a qualitative level, this is observed in Fig. 1(b) as the pressure is increased.

The magnetic resistivity for a hybridizing, CEF split system can be computed following the procedure described by Cornut and Coqblin.[20] Although the calculation is lengthy and cannot be reduced to a small number of equations, all the different steps of the calculation are well described in Ref. 20. This allows us to determine the pressure evolution of the magnetic exchange energy $J_{ex}$ between conduction and localized 4$f$ electrons. This model applies to alloys and compounds with cerium impurities and considers the influence of the crystalline field on the Kondo effect. The scattering of conduction electrons with the ground state and excited states, due to the CEF effect, of cerium impurities is considered. The Cornut and Coqblin calculation has also been applied to cerium compounds such as $CeAl_2$,[29] $CeAl_3$,[43] and qualitatively to $Ce_3Pt_4In_{13}$.[38] Although $CeZn_{11}$ orders below 2 K and cannot truly be considered as a dilute alloy, the concentration of cerium in $CeZn_{11}$ is rather small ($c \approx 8.33$ at.%). Moreover, the magnetic properties at high temperatures are well understood assuming a local character of the 4$f$ electrons. In addition, coherence effects are expected to be negligible at high temperatures. We therefore fit our data above 20 K, but keeping in mind that the lower temperature range is not expected to be perfectly reproduced by this model. The physical constants and assumptions are given in Ref. 20, and the free parameters of the calculation are the following: a direct scattering potential $\upsilon$, the matrix element of mixing between 4$f$ and conduction electrons at the Fermi level $V_{k_F}$, the density of states at the Fermi energy $E_F$ for the one spin direction $n(E_F)$, the energy of the ground state $E_0$ measured from $E_F$, the energy gap between the ground state and the excited CEF levels $\Delta_1$ and $\Delta_2$, and a cutoff energy $D$. In order to reduce the number of fitting parameters, we assume that all the magnetic exchange energies $J_{MM'}$ are equal (and referred to as $J_{ex}$). This removes the dependence on $V_{k_F}$ and $E_0$. We also consider that $n(E_F)$ is pressure independent. An estimate of $n(E_F)$ can be obtained from the free electron expression $\mathcal{N}(E_F) = \frac{3}{2}\frac{N}{E_F}$ where $N$ is the

number of electrons taken as three electrons per cerium. The Fermi energy can be obtained in the free electron model from the carrier density of $\sim 4.4 \times 10^{28}$ m$^{-3}$ at 300 K obtained from Hall resistivity measurements in the one-band approximation.[7] This gives $E_F \approx 4.5$ eV. Another estimation can be made from the thermoelectric power (TEP) measurements. As mentioned in Ref. 7, the temperature dependence of the TEP is almost linear above 125 K. At high temperatures, the TEP is given by $S = \frac{\pi^2}{e}\frac{k_B^2}{E_F}T$ for hole-type carriers,[44] where $-e$ is the electron charge and $k_B$ is the Boltzmann constant. A linear fit of the data above 125 K gives a slope of 0.0156 $\mu$V K$^{-2}$ which leads to $E_F \approx 4.7$ eV, in good agreement with the estimate from the Hall resistivity. From these values for $E_F$, we deduce that $n(E_F) \approx 0.5$ state/eV atom. Another parameter of the Cornut and Coqblin model is the direct scattering potential $\upsilon$, which is difficult to estimate: its evaluation comes essentially from the low-temperature behavior of $\rho$ but the model is not valid in this region mainly because of coherence effects. $|\upsilon|$ is expected to be of the order of $|J_{ex}|$ and we have chosen $|\upsilon| = 0.2$ eV, independent of pressure (a similar value is taken in other cerium compounds).[20,29,43] Finally, since we fit our data only above 20 K, we take the gap energy of the first excited level due to the CEF effect fixed to $\Delta_1 = 14$ K. The remaining free parameters of the calculation are therefore the exchange energy $J_{ex}$, the cutoff energy $D$, and the gap energy $\Delta_2$ due to the CEF effect. The results of the fit for different pressures are represented as dashed lines in Fig. 1(b). The temperature dependence is well reproduced and, in particular, the changes of slopes at the CEF energies. As expected, the agreement is better in the higher temperature range, which further confirms the fact that the cerium can be considered as a local diluted impurity. The fitting parameters are presented in Fig. 2. As already mentioned in Refs. 20 and 29, the variation of the theoretical parameter $D$ under pressure is not physically important. More importantly, Fig. 2 shows that the absolute value of the magnetic exchange energy $|J_{ex}|$ increases with pressure as is usual for Kondo systems.[45] The pressure dependence of $J_{ex}$ is linear and $\frac{d|J_{ex}|}{dp} \approx 14$ meV/GPa. This value for $CeZn_{11}$ can be compared to $Ce_3Pt_4In_{13}$ ($\frac{d|J_{ex}|}{dp} \approx 8.4$ meV/GPa), which orders antiferromagnetically below 0.95 K.[38] It would be interesting to compare these values to other cerium compounds, especially members of the $CeT_2(Si,Ge)_2$ ($T$ = Cu,Pd,Au).[31–35] The knowledge of the pressure dependence of $J_{ex}$ will be used later to estimate the variation of the magnetic ordering temperature $T_{O_1}(p)$. We note that fitting down to 5 K with $\Delta_1$ as a free parameter gave essentially the same estimate of the variation of the magnetic ordering temperature $T_{O_1}(p)$, and values for $\Delta_1$ between 14 and 18 K. However, as already mentioned, the data are not well reproduced at low temperatures. We also note that the value obtained for $\Delta_2 \approx 100$ K is higher than the one obtained from specific heat measurements,[7,12] which were, however, limited to below 20 K. Inelastic neutron scattering experiments would be helpful in order to confirm the CEF level scheme of $CeZn_{11}$.

We now focus on the low-temperature ordered phase. Figure 3(a) shows the low-temperature dependence of the electrical resistivity at different pressures. The corresponding temperature derivatives are presented in Fig. 3(b). At ambient pressure, the ordering temperature $T_{O_1}$, which is associated with antiferromagnetism,[7] is characterized by a rapid loss

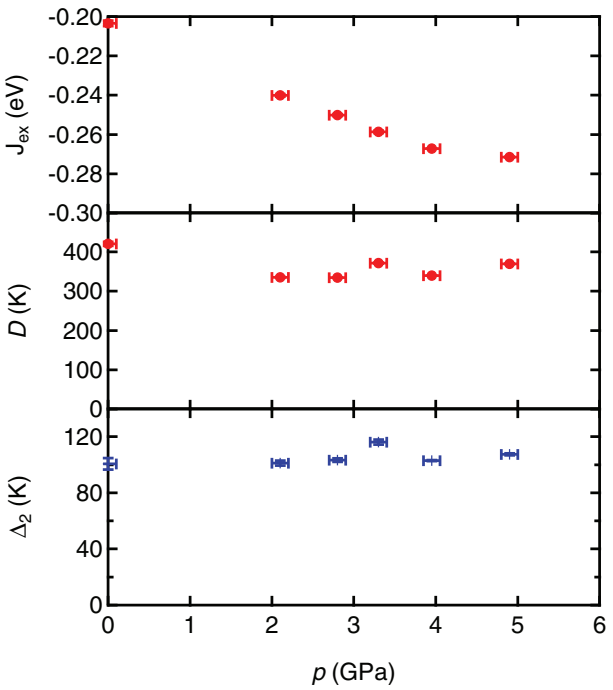


FIG. 2. (Color online) Pressure dependence of the exchange energy $J_{ex}$, the cutoff energy $D$ and the gap energy $\Delta_2$ due to the CEF effect obtained from the fits of $\rho - \rho_{LaZn_{11}}$ [see Fig. 1(b)] within the Cornut and Coqblin model.[20]

of electrical resistivity in Fig. 3(a), or more clearly by a peak in $d\rho/dT$ in Fig. 3(b). Such behavior is expected in magnetic metals where the resistivity due to spin disorder scattering is reduced in the ordered phase.[46] We define the ordering temperature $T_{O_1}$ as the middle point of the sharp rise in $d\rho/dT$ as illustrated in Fig. 3(b) for the data at 3.3 GPa. With applied pressure, a second peak is visible in $d\rho/dT$, indicating the appearance of a new phase at $T_{O_2}$, which most likely corresponds to a transition to a different type of magnetic order. We define the ordering temperature $T_{O_2}$ as the peak position in $d\rho/dT$ as illustrated in Fig. 3(b) for the data at 3.3 GPa by a circle. Due to the finite initial pressure step, which was necessary to ensure the sealing of the

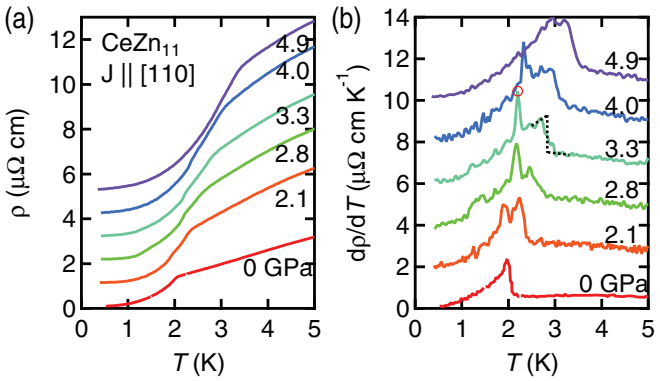


FIG. 3. (Color online) Temperature dependence of the electrical resistivity (a) and its temperature derivative (b) at different pressures. For clarity, the data are offset by increments of 1 $\mu\Omega$cm in (a) and of 2 $\mu\Omega$ cm K$^{-1}$ in (b). The criteria for determination of $T_{O_1}$ and $T_{O_2}$ are shown for the $p = 3.3$ GPa curve in (b) and discussed in the text.

pressure cell, the pressure at which the new phase appears is not precisely known. Our measurements show that this pressure must be below 2.1 GPa. Such multiple magnetic transitions are frequently revealed upon cooling in rare-earth intermetallic compounds,[47,48] and can sometimes be found in Ce compounds: CeRuSiH (Ref. 49), $CeRu_2Ge_2$ (Refs. 50–52), $CeRu_2Al_2B$ (Ref. 53), and of course, CeSb (Refs. 54 and 55), for example. Such a series of transitions is also observed in some uranium based compounds, and in particular in $UCd_{11}$ (Ref. 56). It is interesting to note that the sharp rise in $d\rho/dT$ at $T_{O_1}$ is of similar shape as the anomaly in specific heat[7] as expected for a second-order magnetic transition.[57] On the other hand, the anomaly in $d\rho/dT$ at the pressure induced transition $T_{O_2}$, especially for $p = 2.8$, 3.3, and 4.0 GPa, is much more symmetric, suggesting a first-order transition. Indeed, the anomaly in specific heat at a second-order phase transition is usually not symmetric showing one behavior on one side, and a different behavior on the other side. However, in the case of a first-order transition, it is the entropy which is discontinuous, and, consequently, the specific heat shows like a broadened Dirac $\delta$ function resembling a more symmetric peak.

The temperature versus pressure phase diagram is shown in Fig. 4. The temperatures of both anomalies increase with pressure up to 4.9 GPa. In the case of a first-order transition, as it might be the case at $T_{O_2}$, the pressure variation of the ordering temperature is given by the Clausius-Clapeyron relation:

$$\frac{dT_{O_2}}{dp} = \frac{\Delta V}{\Delta S}, \tag{1}$$

where $\Delta S$ is the discontinuity of entropy and $\Delta V$ is the discontinuity in volume. Assuming that $\Delta S > 0$, our observation that $dT_{O_2}/dp > 0$ implies $\Delta V > 0$. Thermal expansion measurements under pressure would be necessary to further discuss the order of the phase transition.

The fact that both anomalies increase with pressure up to 4.9 GPa indicates that $CeZn_{11}$ is far from a pressure induced quantum critical point. Assuming that the magnetic order is mediated through the RKKY interaction,[59–61] we have $T_{\mathrm{RKKY}} \propto J_{\mathrm{ex}}^2$. We can use the $J_{\mathrm{ex}}(p)$ values determined from the high-temperature dependence of the resistivity to derive the variation of the ordering temperature with pressure. This is represented by a dashed line in Fig. 4. The increase of $T_{O_1}$ with pressure is rather well reproduced by this crude estimate. Given all the approximations that we have mentioned previously, the agreement is remarkably good.

We can also calculate the single impurity Kondo temperatures within the Cornut and Coqblin model. In this model, the single impurity Kondo temperature $T_{K0}^n$ corresponding to a temperature regime where $n$ energy multiplets are occupied is:[20]

$$T_{K0}^n = D^{(n)} \exp\left[-\frac{1+\frac{\upsilon^2}{J_{\mathrm{ex}}^2}\frac{(2j+1)\lambda_n}{\lambda_n^2-1}}{\lambda_n |J_{\mathrm{ex}}| n(E_F)}\right], \tag{2}$$

where $j$ is the total angular momentum quantum number, $\lambda_n$ is the total degeneracy of the $n$ occupied energy levels, and $D^{(n)}$ is an effective cutoff (the formula given in Ref. 20 was corrected in Ref. 58):

$$D^{(n)} = \frac{\frac{D}{2.4}}{\prod_{i=1}^{n}\prod_{l=n+1}^{N}\left|\frac{\Delta_{li}}{\frac{D}{1.85}}\right|^{\frac{\alpha_i\alpha_l}{\lambda_n^2}}}, \tag{3}$$

where $\alpha_i$ is the degeneracy of the level $i$, $N$ is the total number of energy multiplets, and $\Delta_{li}$ is the energy gap between the two levels $i$ and $l$. In the case of $Ce^{3+}$ ion in tetragonal point symmetry, $j = \frac{5}{2}$ and $N = 3$. The pressure dependencies of the three single-impurity Kondo temperatures are shown in Fig. 5(a). We note that these values are dependent on our estimation of $n(E_F)$ and $|\upsilon|$. $T_{K0}^{\mathrm{high}}$ is the single impurity Kondo temperature for the high-temperature regime where all the six states of a $Ce^{3+}$ ion are occupied. It is not reached experimentally because, upon cooling, the second excited energy level starts to be depopulated before the system reaches $T_{K0}^{\mathrm{high}}$. The same remark applies for $T_{K0}^{\mathrm{int}}$, which is

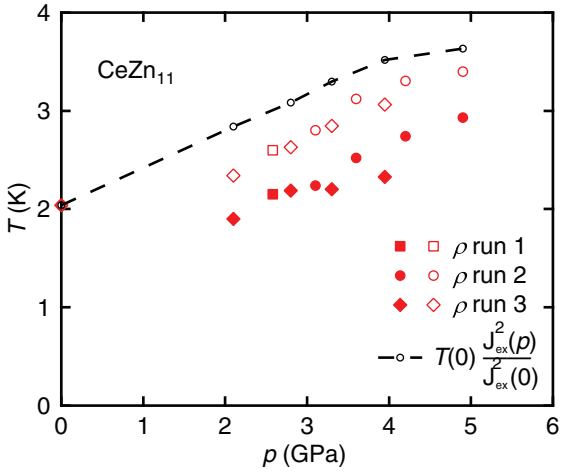


FIG. 4. (Color online) Temperature vs pressure phase diagram of $CeZn_{11}$ determined from resistivity measurements. The dashed line represents an estimate of $T_{O_1}$ from the pressure dependence of the magnetic exchange energy $|J_{\mathrm{ex}}|$ shown in Fig. 2. Data from three separate pressure cell runs are shown.

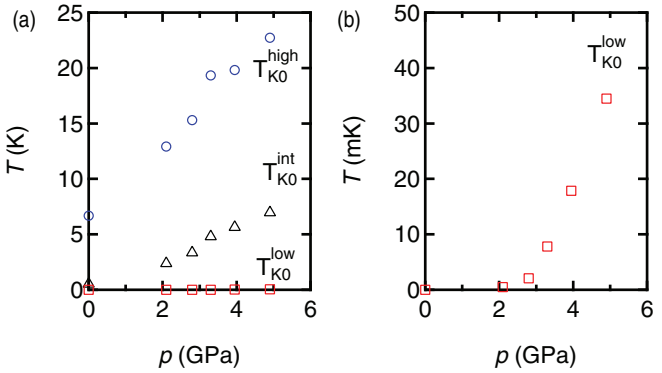


FIG. 5. (Color online) Pressure dependence of the single impurity Kondo temperature $T_{K0}$ for different numbers of occupied energy multiplets, calculated from the Cornut and Coqblin model[20,58] (see text). $T_{K0}^{\mathrm{high}}$ is the single impurity Kondo temperature for the high-temperature regime where all the six states of a cerium ion are occupied, $T_{K0}^{\mathrm{low}}$ is for the low-temperature regime where only the ground-state doublet is occupied, and $T_{K0}^{\mathrm{int}}$ is for an hypothetical intermediate regime where only four states would be occupied.

the single impurity Kondo temperature for an hypothetical intermediate regime where only four states would be occupied, i.e., for $\Delta_1 \ll k_B T \ll \Delta_2$. Finally, the only temperature that could be reached experimentally is $T_{K0}^{\text{low}}$, the single impurity Kondo temperature for the low-temperature regime where only the ground state doublet is occupied. The pressure dependence of $T_{K0}^{\text{low}}$ is shown in Fig. 5(b). Although $T_{K0}^{\text{low}}$ increases rapidly with pressure, it is still much lower than the ordering temperature and it is not reached in our experiments. Below $T_{K0}^{\text{low}}$, a Kondo compensation of the total angular momentum would occur. However, our values of $T_{K0}$ should be considered as very rough estimates and it has to be reminded that coherence effects as well as the effect of the magnetic ordering are not considered in the Cornut and Coqblin model, and, consequently, we fitted our data only above 20 K.

In cerium compounds, pressure drives the system towards the right side of the Doniach phase diagram,[5,6] i.e., from the region where the RKKY interaction dominates to the region where it is the Kondo effect that dominates. We expect that at

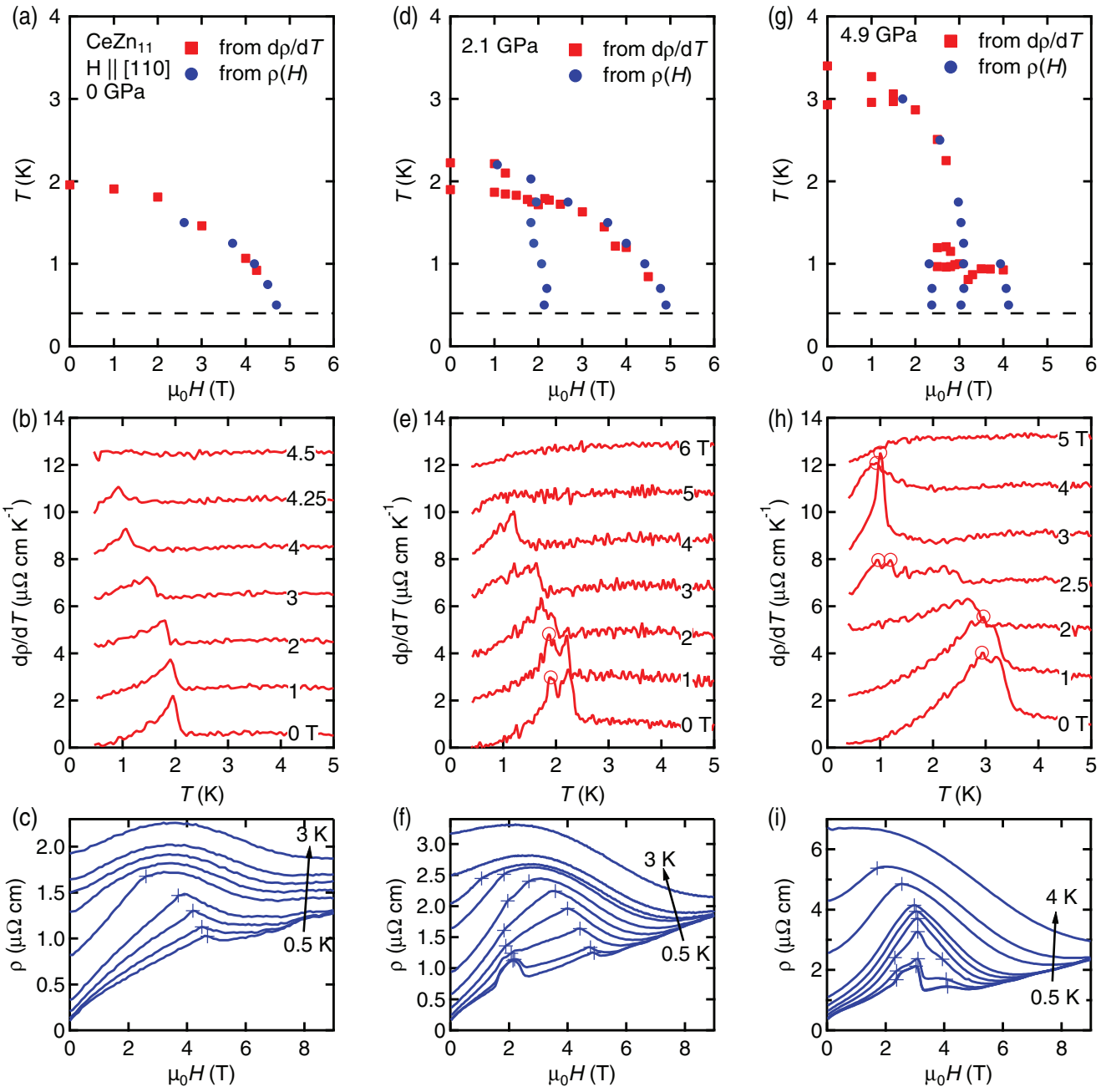


FIG. 6. (Color online) Temperature vs magnetic field phase diagram at three different pressures: (a)–(c) ambient pressure, (d)–(f) 2.1 GPa, and (g)–(i) 4.9 GPa. Each of these phase diagrams is constructed from anomalies in the temperature dependence of $d\rho/dT$ shown in (b), (e), and (h) {middle point of the sharp rise in $d\rho/dT$ [see Fig. 3(b) for the data at 3.3 GPa] and local maxima marked as circles}; and also from the anomalies (local maximum, change of slope, maximum in $d\rho/dH$) in the magnetic field dependence of the resistivity at different temperatures indicated by + in (c), (f), and (i). Data in (b), (e), and (h) are offset by increments of 2 $\mu\Omega$ cm $K^{-1}$.

higher pressure, the Kondo effect will become more significant and will compete more strongly with the RKKY interaction, leading to a decrease of the magnetic ordering temperature. With increasing pressure, we do not observe any increase of the deviation of the ordering temperature from the estimation. Therefore we conclude that the influence of the Kondo effect on the magnetic ordering temperature is still small, even at our highest pressure of 4.9 GPa. This is consistent with the fact that the single impurity Kondo temperature $T_{K0}^{\mathrm{low}}$ is still much lower than the ordering temperature, so that the energy scale for the Kondo compensation of the magnetic moments is still small.

We will now focus on the field dependence of the resistivity anomaly. Three different cases are presented in Fig. 6 : $p = 0$ (a)–(c), 2.1 (d)–(f), and 4.9 GPa (g)–(i).

In Fig. 6(b), at ambient pressure, only one ordering transition is observed as a positive peak in $d\rho/dT$. An applied magnetic field along the [110] axis reduces the ordering temperature $T_{O_1}$. The anomaly can also be observed in the magnetic field dependence of the resistivity at different temperature [see Fig. 6(c)]. The resulting phase diagram is presented in Fig. 6(a) and is consistent with the one obtained from magnetization and specific heat measurements.[7]

Figure 6(e) shows $d\rho/dT$ for $p = 2.1$ GPa. At zero field, two peaks in $d\rho/dT$ indicate the two transitions. With increasing $H$, the two transitions seem to merge at around 2 T. With further increases of the magnetic field, the anomaly is suppressed down to lower temperatures and disappears near 5 T. The magnetic field dependence of the resistivity [see Fig. 6(g)] shows a local maximum at low temperature around 2 T. This anomaly evolves into a kink at higher temperature. The phase diagram is shown in Fig. 6(d). The anomalies seen in the resistivity data allow us to separate three different domains in the phase diagram in addition to the paramagnetic region.

At the highest pressure reached in this study, 4.9 GPa, the two anomalies are less distinguishable in $d\rho/dT$. They still merge with applied magnetic field [see Fig. 6(h)]. At 2.5 T, a new anomaly is visible as a local maximum around 1 K. It becomes very sharp at 3 T, then it broadens at higher magnetic field and finally disappears above 4 T. The phase diagram shown in Fig. 6(g) is even more complex than the one at lower pressures. Such a phase diagram is reminiscent of quantum critical behavior, where new phases are observed in close proximity to the quantum phase transition.

$CeZn_{11}$ belongs to a small group of Ce-based compounds in which a fine tuning of the exchange interaction can be achieved by temperature, applied magnetic field, and/or pressure to drive the system into various magnetic ground states. Other compounds with complex magnetic phase diagrams include CeSb,[54,55] $CeRu_2Ge_2$,[50–52] $CeRhIn_5$,[62,63] $CeCd_{11}$,[64] and $CeRu_2Al_2B$.[53] Interestingly, the uranium compound, $UCd_{11}$, also shows a complicated $T$-$p$-$H$ phase diagram,[65] however, elastic neutron scattering experiments failed to determine the magnetic structure.[66] In $UCd_{11}$, the boundaries between different phases seem to cross each other[56,67] in a very similar way as what we observe in $CeZn_{11}$ at 2.1 GPa, for example [see Fig. 6(d)]. Assuming that such a $T$-$H$ phase diagram is not a special section of a higher-dimensional phase diagram, the intersection point of such crossing cannot be a point where four non-symmetry-breaking phases coexist, which would not be allowed by Gibbs phase rule. Gibbs phase rule does not apply for phases that involve certain symmetry breaking, or for higher than first-order phase transitions. Griffiths rule[68] can be used for higher-order critical points, but it still does not apply if the phases break certain symmetry of the Hamiltonian. Therefore we conclude that in $CeZn_{11}$ under pressure and magnetic field, some of the phases are breaking certain symmetry or/and at least one of the boundary line is of a higher order than a first-order line.

Finally, another peculiarity of $CeZn_{11}$ indicates the complexity of the magnetism in this material. It has been shown that the ordering temperature $T_{O_1}$ increases with pressure, in qualitative agreement with the increase of the exchange energy $|J_{\mathrm{ex}}|$ (see Fig. 4). One then expects the critical magnetic field to increase as well. However, the phase diagrams in Figs. 6(a), 6(d), and 6(h) show that this is not the case for $CeZn_{11}$. This can also be seen in Fig. 7, which shows the magnetic field dependence of the resistivity at different pressures: the critical magnetic field at $H_1$ decreases with pressure, although $T_{O_1}$ increases.

In $CeRhIn_5$, the complex magnetic phase diagram includes spiral magnetic order.[69] Such order can result from the frustration between two competing interactions when the coupling between nearest neighbors $J_1$ and next-nearest neighbors $J_2$ are of opposite sign.[70] In $CeZn_{11}$, anisotropic susceptibility measurements have indicated Curie-Weiss temperatures $\theta_{[100]} \approx +1.2$ K, whereas $\theta_{[110]} \approx -1.6$ K and $\theta_{[001]} \approx -31$ K,[7] although such anisotropy could also arise from the CEF effect. The influence of frustration on quantum criticality was recently pointed out by several authors.[71–74] The complex magnetic phase diagrams might also be a consequence of CEF levels crossing due to the Zeeman effect on the ground state and the first excited CEF level. In tetragonal point symmetry, the eigenfunctions $\Gamma_7^{(1)}$ and $\Gamma_7^{(2)}$ are linear combinations of the eigenfunctions of the free ion. It is therefore difficult to estimate the Zeeman splitting without more knowledge of the wave functions of the energy levels. In the case of $CeZn_{11}$, the origin of the rich phase diagrams is still unclear: frustrated

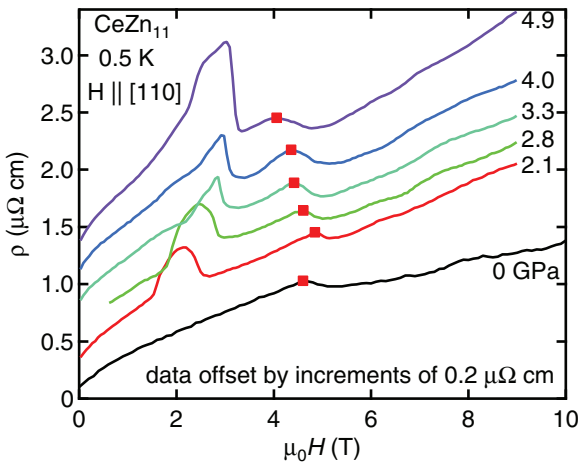


FIG. 7. (Color online) Magnetic field dependence of the electrical resistivity at different pressures. The critical field $H_1$ is revealed by a kink in the magnetoresistance (red squares). Although the ordering temperature increases with applied pressure, the critical field $H_1$ decreases.

competing interactions, proximity of quantum criticality and low CEF levels might contribute to the complexity; further experiments are certainly required.

In summary, we have measured the electrical resistivity of $CeZn_{11}$ under pressure up to 5 GPa, and magnetic field up to 9 T. The high-temperature part of the electrical resistivity is well described by the combination of the Kondo and the CEF effects. We were able to extract the pressure dependence of the magnetic exchange interaction $J_{ex}$ between conduction and localized $4f$ electrons. The pressure dependence of the ordering temperature is qualitatively well reproduced by the pressure dependence of $J_{ex}$. With applied pressure, the magnetic ordering temperature increases, indicating that $CeZn_{11}$ is on the left side of the Doniach diagram, where the RKKY interaction dominates over the Kondo effect. In addition, rich magnetic phase diagrams have been determined from electrical resistivity measurements under high pressure and magnetic fields for $H \parallel [110]$, revealing that the magnetic ordering of $CeZn_{11}$ is not simple under pressure. We hope that the present work will stimulate further experiments to investigate the properties of this material.

## ACKNOWLEDGMENTS

We would like to thank M. A. Tanatar, A. Jesche, D. K. Finnemore, A. Kreyssig, and R. Flint for useful discussions. This work was carried out at the Iowa State University, and V.T. was supported by the AFOSR-MURI grant No. FA9550-09-1-0603. Part of this work was performed at the Ames Laboratory, US DOE, under Contract No. DE-AC02-07CH11358.

*taufour@ameslab.gov

[1] G. R. Stewart, Rev. Mod. Phys. **56**, 755 (1984).
[2] G. R. Stewart, Rev. Mod. Phys. **73**, 797 (2001).
[3] H. v. Löhneysen, A. Rosch, M. Vojta, and P. Wölfle, Rev. Mod. Phys. **79**, 1015 (2007).
[4] C. Pfleiderer, Rev. Mod. Phys. **81**, 1551 (2009).
[5] S. Doniach, Physica B & C **91**, 231 (1977).
[6] S. Doniach, in *Valence Instabilities and Related Narrow-Band Phenomena*, edited by R. D. Parks (Plenum Press, New York, 1977), pp. 169–176.
[7] H. Hodovanets, S. L. Bud'ko, X. Lin, V. Taufour, M. G. Kim, D. K. Pratt, A. Kreyssig, and P. C. Canfield, Phys. Rev. B **88**, 054410 (2013).
[8] M. S. Torikachvili, S. Jia, E. D. Mun, S. T. Hannahs, R. C. Black, W. K. Neils, D. Martien, S. L. Bud'ko, and P. C. Canfield, Proc. Natl. Acad. Sci. USA **104**, 9960 (2007).
[9] H. Sato, D. Kikuchi, K. Tanaka, H. Aoki, K. Kuwahara, Y. Aoki, M. Kohgi, H. Sugawara, and K. Iwasa, J. Magn. Magn. Mater. **310**, 188 (2007).
[10] B. C. Sales, D. Mandrus, and R. K. Williams, Science **272**, 1325 (1996).
[11] O. Zelinska, M. Conrad, and B. Harbrecht, Z. Krist.-New Cryst. Struct. **219**, 357 (2004).
[12] Y. Nakazawa, M. Ishikawa, S. Noguchi, and K. Okuda, J. Phys. Soc. Jpn. **62**, 3003 (1993).
[13] K. A. Gschneidner, J. Tang, S. K. Dhar, and A. I. Goldman, Physica B **163**, 507 (1990).
[14] J. Tang and K. A. Gschneidner, J. Magn. Magn. Mater. **75**, 355 (1988).
[15] Z. Fisk, G. R. Stewart, J. O. Willis, H. R. Ott, and F. Hulliger, Phys. Rev. B **30**, 6360 (1984).
[16] Y. Hirose, Y. Miura, H. Tsutsumi, S. Yoshiuchi, M. Ohya, K. Sugiyama, T. Takeuchi, H. Yamagami, E. Yamamoto, Y. Haga, R. Settai, and Y. Onuki, Phys. Status Solidi B-Basic Solid State Phys. **250**, 642 (2013).
[17] E. Yamamoto, Y. Hirose, K. Enoki, K. Mitamura, K. Sugiyama, T. Takeuchi, M. Hagiwara, K. Kindo, Y. Haga, R. Settai, and Y. Ōnuki, J. Phys. Soc. Jpn. **81SB**, SB023 (2012).
[18] H. Meyer and P. L. Smith, J. Phys. Chem. Solids **9**, 285 (1959).
[19] S. K. Malik, J. Tang, and K. A. Gschneidner, J. Magn. Magn. Mater. **109**, 316 (1992).
[20] B. Cornut and B. Coqblin, Phys. Rev. B **5**, 4541 (1972).
[21] K. Yamada, K. Yosida, and K. Hanzawa, Prog. Theor. Phys. **71**, 450 (1984).
[22] K. Hanzawa, K. Yamada, and K. Yosida, J. Magn. Magn. Mater. **47-48**, 357 (1985).
[23] E. Colombier and D. Braithwaite, Rev. Sci. Instrum. **78**, 093903 (2007).
[24] A.-S. Rueetschi and D. Jaccard, Rev. Sci. Instrum. **78**, 123901 (2007).
[25] S. K. Kim, M. S. Torikachvili, E. Colombier, A. Thaler, S. L. Bud'ko, and P. C. Canfield, Phys. Rev. B **84**, 134525 (2011).
[26] N. Tateiwa and Y. Haga, Rev. Sci. Instrum. **80**, 123901 (2009).
[27] G. J. Piermarini, S. Block, and J. D. Barnett, J. Appl. Phys. **44**, 5377 (1973).
[28] B. Bireckoven and J. Wittig, J. Phys. E: Sci. Instrum. **21**, 841 (1988).
[29] M. Nicolas-Francillon, A. Percheron, J. Achard, O. Gorochov, B. Cornut, D. Jerome, and B. Coqblin, Solid State Commun. **11**, 845 (1972).
[30] E. Vargoz, P. Link, D. Jaccard, T. Le Bihan, and S. Heathman, Physica B **229**, 225 (1997).
[31] D. Jaccard, J. M. Mignot, B. Bellarbi, A. Benoit, H. F. Braun, and J. Seirro, J. Magn. Magn. Mater. **47-48**, 23 (1985).
[32] P. Link and D. Jaccard, Physica B **230**, 31 (1997).
[33] E. Vargoz and D. Jaccard, J. Magn. Magn. Mater. **177**, 294 (1998).
[34] A. Demuer, A. T. Holmes, and D. Jaccard, J. Phys.-Condes. Matter **14**, L529 (2002).
[35] H. Wilhelm and D. Jaccard, Phys. Rev. B **66**, 064428 (2002).
[36] H. Wilhelm, S. Raymond, D. Jaccard, O. Stockert, H. von Lohneysen, and A. Rosch, J. Phys.-Condes. Matter **13**, L329 (2001).
[37] H. Nakawaki, Y. Inada, R. Asai, M. Yamada, T. Okubo, S. Ikeda, A. Thamizhavel, T. Kobayashi, R. Settai, E. Yamamoto, and Y. Onuki, J. Phys.-Condes. Matter **14**, L305 (2002).
[38] M. F. Hundley, J. L. Sarrao, J. D. Thompson, R. Movshovich, M. Jaime, C. Petrovic, and Z. Fisk, Phys. Rev. B **65**, 024401 (2001).
[39] Y. Kawamura, T. Nishioka, H. Kato, M. Matsumura, K. Matsubayashi, and Y. Uwatoko, Journal of Physics Conference Series **200**, 012082 (2010).
[40] P. K. Das, N. Kumar, R. Kulkarni, and A. Thamizhavel, Phys. Rev. B **83**, 134416 (2011).

[41]H. Hidaka, S. M. Ramos, E. N. Hering, M. B. Fontes, E. B. Saitovitch, S. Otani, T. Wakabayashi, Y. Shimizu, T. Yanagisawa, and H. Amitsuka, J. Phys.: Conf. Ser. **391**, 012019 (2012).
[42]Y. Nishida, A. Tsuruta, and K. Miyake, J. Phys. Soc. Jpn. **75**, 064706 (2006).
[43]A. Percheron, J. C. Achard, O. Gorochov, B. Cornut, D. Jerome, and B. Coqblin, Solid State Commun. **12**, 1289 (1973).
[44]A. H. Wilson, Mathematical Proceedings of the Cambridge Philosophical Society **33**, 371 (1937).
[45]J. S. Schilling, Adv. Phys. **28**, 657 (1979).
[46]N. H. Andersen, in *Crystalline Electric Field and Structural Effects in f-Electron Systems*, edited by J. E. Crow, R. P. Guertin, and T. W. Mihalisin (Plenum Press, New York, 1980), pp. 373–387.
[47]S. L. Bud'ko, Z. Islam, T. A. Wiener, I. R. Fisher, A. H. Lacerda, and P. C. Canfield, J. Magn. Magn. Mater. **205**, 53 (1999).
[48]M. A. Avila, S. L. Bud'ko, and P. C. Canfield, J. Magn. Magn. Mater. **270**, 51 (2004).
[49]B. Chevalier, E. Gaudin, S. Tence, B. Malaman, J. R. Fernandez, G. Andre, and B. Coqblin, Phys. Rev. B **77**, 014414 (2008).
[50]H. Wilhelm, K. Alami-Yadri, B. Revaz, and D. Jaccard, Phys. Rev. B **59**, 3651 (1999).
[51]S. Sullow, M. C. Aronson, B. D. Rainford, and P. Haen, Phys. Rev. Lett. **82**, 2963 (1999).
[52]S. Raymond, P. Haen, R. Calemczuk, S. Kambe, B. Fak, P. Lejay, T. Fukuhara, and J. Flouquet, J. Phys.: Condens. Matter **11**, 5547 (1999).
[53]R. E. Baumbach, H. Chudo, H. Yasuoka, F. Ronning, E. D. Bauer, and J. D. Thompson, Phys. Rev. B **85**, 094422 (2012).
[54]J. Rossat-Mignod, P. Burlet, J. Villain, H. Bartholin, W. Tchengsi, D. Florence, and O. Vogt, Phys. Rev. B **16**, 440 (1977).
[55]T. A. Wiener and P. C. Canfield, J. Alloy. Compd. **303**, 505 (2000).
[56]D. Aoki, T. Inoue, K. Kindo, N. Suzuki, K. Miyake, Y. Inada, R. Settai, K. Sugiyama, E. Yamamoto, Y. Haga, and Y. Onuki, J. Phys. Soc. Jpn. **68**, 3117 (1999).
[57]M. Fisher and J. Langer, Phys. Rev. Lett. **20**, 665 (1968).
[58]A. K. Bhattacharjee and B. Coqblin, Phys. Rev. B **38**, 338 (1988).
[59]M. A. Ruderman and C. Kittel, Phys. Rev. **96**, 99 (1954).
[60]T. Kasuya, Prog. Theor. Phys. **16**, 45 (1956).
[61]K. Yosida, Phys. Rev. **106**, 893 (1957).
[62]A. L. Cornelius, P. G. Pagliuso, M. F. Hundley, and J. L. Sarrao, Phys. Rev. B **64**, 144411 (2001).
[63]G. Knebel, D. Aoki, D. Braithwaite, B. Salce, and J. Flouquet, Phys. Rev. B **74**, 020501 (2006).
[64]S. Yoshiuchi, T. Takeuchi, M. Ohya, K. Katayama, M. Matsushita, N. Yoshitani, N. Nishimura, H. Ota, N. Tateiwa, E. Yamamoto, Y. Haga, H. Yamagami, F. Honda, R. Settai, and Y. Onuki, J. Phys. Soc. Jpn. **79**, 044601 (2010).
[65]J. D. Thompson, Z. Fisk, M. W. McElfresh, H. R. Ott, and M. B. Maple, Phys. Rev. B **39**, 2578 (1989).
[66]J. D. Thompson, A. C. Lawson, M. W. McElfresh, A. P. Sattelberger, and Z. Fisk, J. Magn. Magn. Mater. **76-77**, 437 (1988).
[67]C. R. Rotundu, B. Andraka, G. R. Stewart, Y. Takano, and Z. Fisk, J. Appl. Phys. **97**, 10A912 (2005).
[68]R. B. Griffiths, Phys. Rev. B **12**, 345 (1975).
[69]N. J. Curro, P. C. Hammel, P. G. Pagliuso, J. L. Sarrao, J. D. Thompson, and Z. Fisk, Phys. Rev. B **62**, R6100 (2000).
[70]H. Kawamura, J. Phys.: Condens. Matter **10**, 4707 (1998).
[71]S. Burdin, D. R. Grempel, and A. Georges, Phys. Rev. B **66**, 045111 (2002).
[72]Q. M. Si, Physica B **378-380**, 23 (2006).
[73]M. Vojta, Phys. Rev. B **78**, 125109 (2008).
[74]P. Coleman and A. H. Nevidomskyy, J. Low Temp. Phys. **161**, 182 (2010).